Journal of Physics: Conference Series **181** (2009) 012072 doi:10.1088/1742-6596/181/1/012072

Finite element prediction of the ultimate axial load capacity of V-section band clamps

S M Barrans[1] and M Muller[1]

[1] University of Huddersfield, School of Computing and Engineering, Queensgate, Huddersfield, HD1 3DH, UK

E-Mail: s.m.barrans@hud.ac.uk

Abstract. Band clamps with a flat bottomed V-section are used to connect a pair of circular flanges to provide a joint with significant axial strength. Despite the wide application of V-band clamps, their behaviour is not fully understood and the ultimate axial strength is currently only available from physical testing. This physical testing has indicated that the ultimate strength is determined by two different types of structural deformation, an elastic deformation mode and a plastic deformation mode. Initial finite element analysis work has demonstrated that analysis of this class of problem is not straightforward. This paper discusses the difficulties encountered when simulating this type of component interaction where contact is highly localised and contact pressures are high.

1. Introduction

V-section band clamps are used in a wide range of applications in the aerospace and automotive industries. As stated by Shoghi [1] they were invented during the Second World War by the Marmon Corporation and are nowadays used to connect together the housings of diesel engine turbochargers and also to assemble satellites to their launching device [2]. The process of assembling V-band clamps to a pair of circular flanges has recently been investigated using classical analysis [3], finite element analysis [4] and experimental validations [5]. Figure 1 shows a V-section band clamp assembled to a pair of flanges in an experimental test rig.

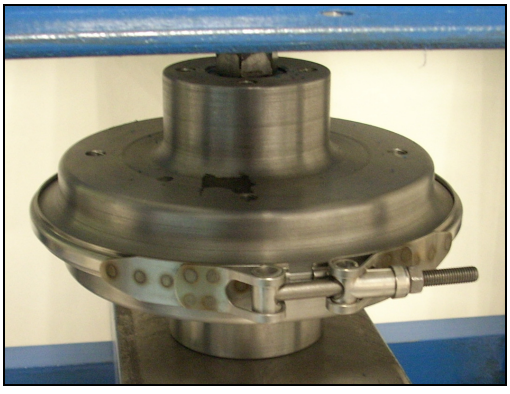

Figure 1: V-section band clamp assembled to a pair of circular flanges for initial experimental testing

Despite their wide application, once assembled to a pair of flanges little is known about the interaction between flange and band. Moreover the failure mode of V-band clamps when undergoing

an axial load is not fully understood. Work has therefore been initiated to generate a finite element model able to predict the ultimate axial load capacity and deformation of V-band Clamps.

2. Initial Finite Element Analyses

To get a first understanding of the structural behaviour of V-band clamps initial finite element analyses were generated using the package ABAQUS. The bands were approximated as being axisymmetric and the plane of symmetry between the two flanges was used to reduce the model size. Whilst Shoghi [1] has demonstrated that the contact load between the bands and flanges is not uniform around the band, the load variation was judged to be small for this first approximation. A sliding contact interaction between the flange and the band clamp was defined and to simulate tightening of the band, it was shrunk on to the flanges. The band clamp was meshed with 2D axisymmetric linear plain strain elements with reduced integration as suggested by Dassault Systems [6] because as observed by Konter [7], second order elements do not distribute the contact pressure uniformly between the mid-side and corner nodes. No meshing was needed for the flange because it was set up as an analytical rigid body. For these initial analyses an implicit solver and a penalty contact algorithm were used with the knowledge that penalty contacts tend to converge more easily and to be more stable as stated by Konter [8].

The material for the band clamp was AISI 304 stainless steel, with a Young's Modulus of 227 GPa, and a Poisson's Ratio of 0.29. The material was modelled as being elastic-plastic with the hardening approximated as linear as explained by Dixit and Dixit [9]. Material data was taken from experimental tests carried out by Shoghi [1]. Using Ludwik's theorem as presented by Meyer [10] these were transformed from engineering to true stress and strain values.

These finite element analyses were set up for a range of different flange diameters, D_f, from 55 mm to 2000 mm with a flange contact edge radius R of 0.1 mm. In practice flange contact radii vary from 0.1 to 0.7 mm. Dassault Systems [11] state that the contact algorithm in ABAQUS requires that the master surface should not contain sharp edges. In the first step of each analysis a boundary condition (BC) was applied to the band at its symmetrical edge to prevent it from moving in the axial direction as shown in Figure 2.

The flange was restrained at its reference point (RP) to prevent it from moving in the radial and axial directions and to prevent it from rotating. Initially there was a gap of about 0.1 mm between the band and the flange. The band was then shrunk onto the flange using an applied reduction in temperature to generate a thermal contraction. This was done to simulate the assembly procedure of tightening the T-bolt nut, which generates an axial load. Using several steps the flange was then moved in the axial direction to simulate a failure of the V-band clamp joint. For these contact interactions the V-band clamp was set as the deformed slave-surface and the flange was set to be the deforming rigid, master-surface. Throughout this paper only the flange diameter D_f rather than the band clamp diameter D_b is used because D_b highly depends on the T-bolt load. After performing these analyses the maximum value of the reaction force in the axial direction at the flange's reference point (RP) could be recorded. This represents the ultimate axial load capacity of the joint. These results are summarized in Figure 3 which indicates that the highest load capacity exists with a flange diameter, D_f of 250 mm.

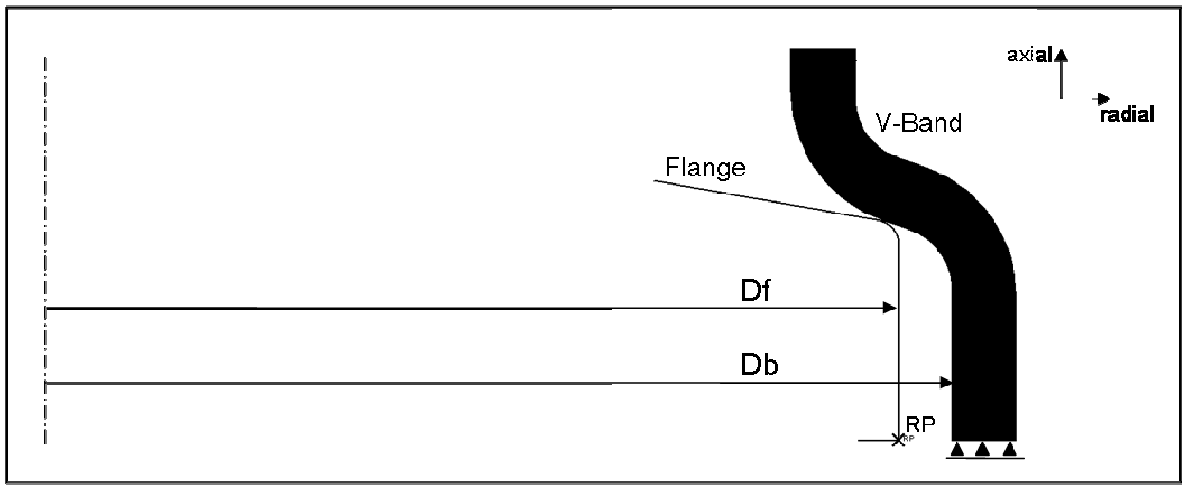

Figure 2: Axisymmetric model arrangement.

It is worth mentioning at this point that these initial analyses were carried out with no friction, a single edge contact radius, R, and a relatively low mesh density using a free, unstructured mesh.

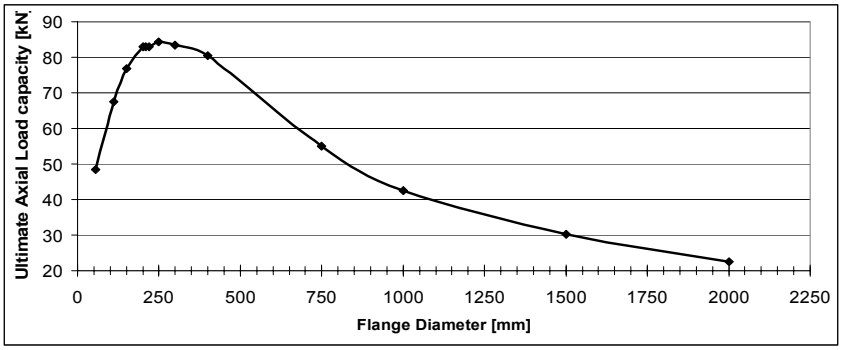

Figure 3: Predicted Axial Load Capacity of V-Section Band Clamps over varying Flange Diameters for Initial FE-Analyses.

3. Implicit Analysis

Using a fixed flange diameter D_f = 250 mm, analyses were carried out for coefficients of friction of 0 and 0.3, for contact edge radii R of 0.3 and 0.5 mm, and for several element thicknesses along the sliding contact surface. Although a contact edge radius of 0.1 mm was used in the initial analyses, these analyses failed with a coefficient of friction of 0.3 and a change in mesh density applied.

3.1. Axial Load Capacity

The analyses generated appeared to be highly dependent on the mesh type and mesh element thickness especially along the contact sliding surface. Figure 4 shows the results for the ultimate axial load capacity for a model with R = 0.5 mm and a coefficient of friction μ of 0.3. As can be seen in this figure the graph for the structured mesh seems to converge to a certain load value for decreasing element size. The graph for the free mesh oscillates with decreasing element size.

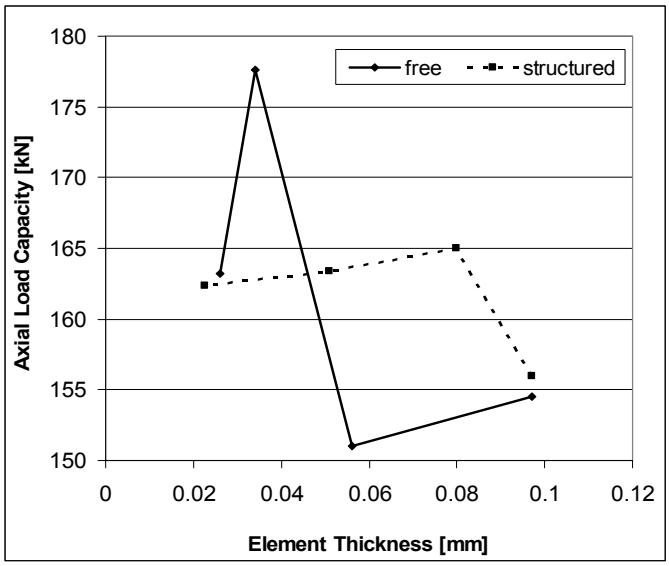

Figure 4: Axial Load Capacity depending on Element Thickness for free and structured mesh, μ = 0.3 and R = 0.5 mm.

Figure 5 indicates the problems that occurred during this analysis work and therefore needed further investigation. Figure 5a shows the axial reaction force at the flange reference point. The very high peak at 255 kN is clearly erroneous. The relative positions of flange and band at this peak are shown in Figure 5b. It can be seen that once the flange starts to slide the elements along the band clamp surface become heavily deformed, especially as the flange slides over the surface. In further analyses these erroneous peaks were noted but were not reported as ultimate axial load capacity. Ignoring this peak, the ultimate axial load capacity of this model is 162 kN.

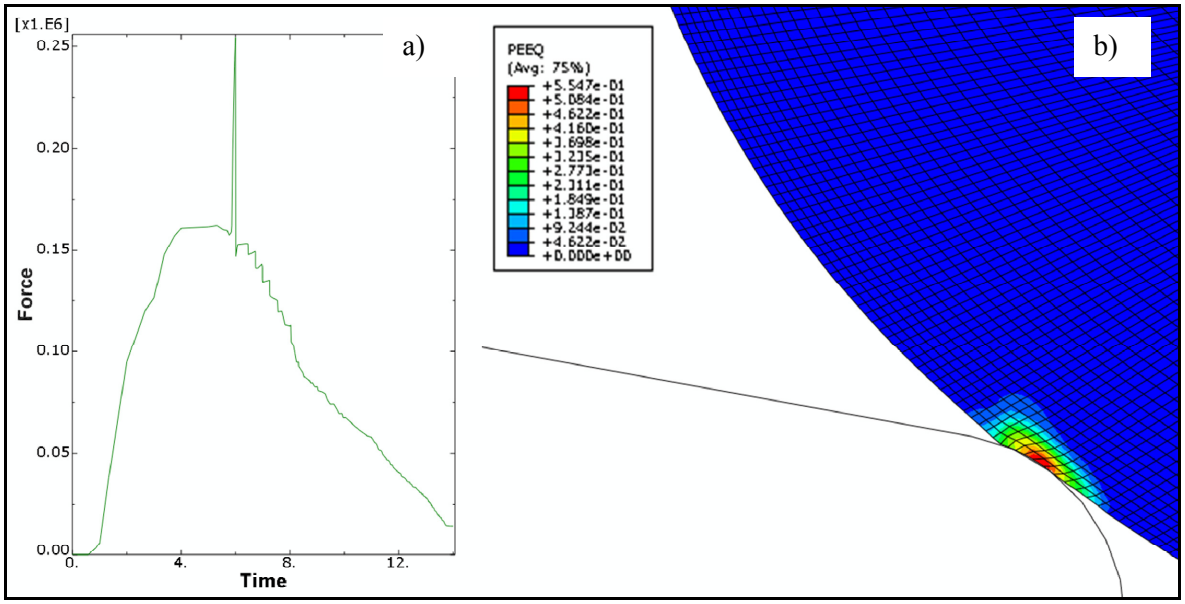

Figure 5: Results for R = 0.5 mm, μ = 0.3, structured mesh, high mesh density a) Axial load at reference point during failure b) position of flange at peak axial load.

Figure 6 shows the results for the same model but with a free, unstructured mesh with nearly the same element size. Again, there is an erroneous peak at the same position in the failure process but it is just at 175kN (Figure 6a), whereas the more reliable axial load capacity seems to be at 163kN almost the same as for the structured mesh. Figure 6b also indicates the same phenomenon of elements starting to deform as the flange starts to slide.

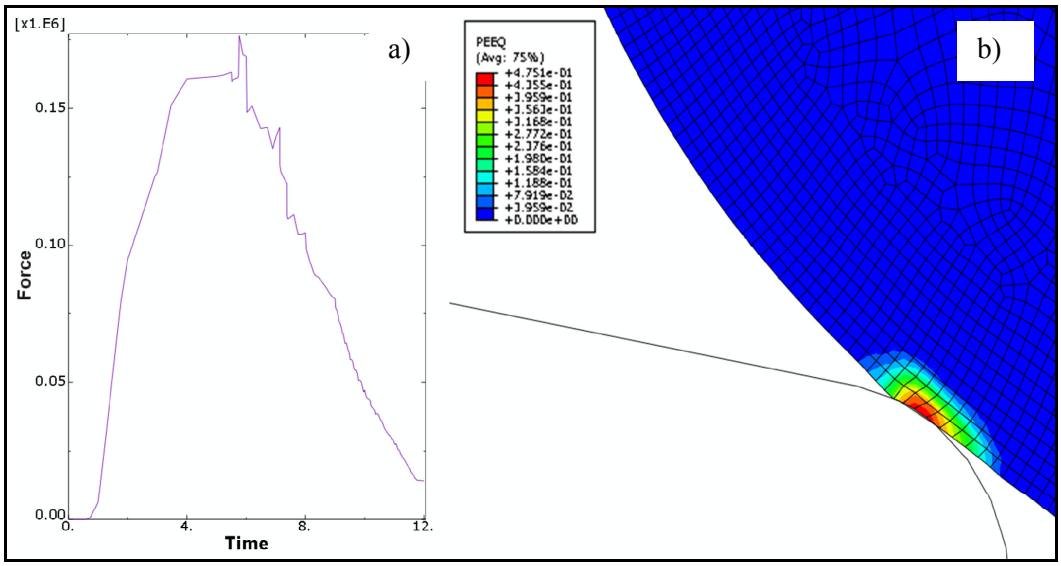

Figure 6: Results for R = 0.5 mm, μ = 0.3, free mesh, high mesh density a) graph of axial load during failure, b) detailed view of position of flange at axial load.

In both cases mentioned above the peak axial load capacity occurs before the flange starts to slide. This shows that as soon as plastic deformation starts in the V-band material, as shown in Figure 5b the ultimate axial load capacity has been reached. This phenomenon has also been seen for models with R = 0.5 mm and μ = 0.

3.2. Plastic Strain

In this section the effect of element thickness along the contact sliding surface of the V-section band clamp on the development of plastic strain in the band clamp will be analysed, for a model with R = 0.3 mm and μ = 0.3. Unlike the models for R = 0.5 mm these models generated many more problems. Figure 7 identifies the position on the contacting surface of the maximum plastic strain ε_{ps}. These values are shown in Figure 8. The two graphs show that the maximum plastic strain increases as the element size decreases. This is due to the one integration point of the reduced integrated linear elements getting closer to the contacting surface, giving much more accurate results. The two meshing methodologies can be seen to give very similar results.

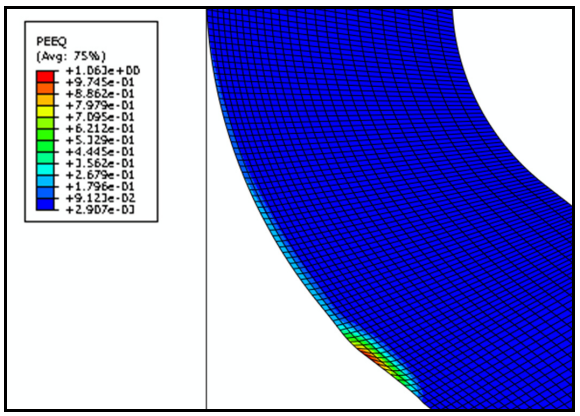

Figure 7: Plastic strain development at contact surface.

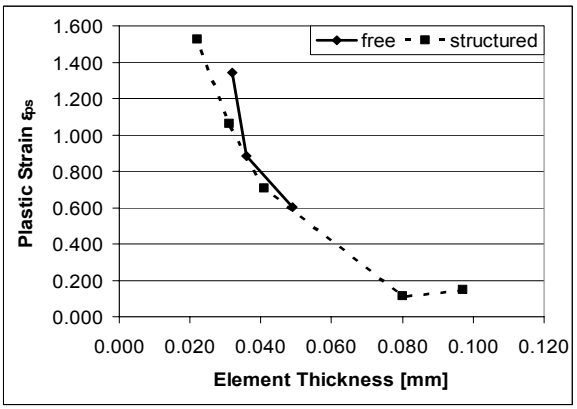

Figure 8: Maximum plastic strain along contact sliding surface for free and structured mesh for R = 0.3 mm and μ = 0.3.

The peak plastic strain described above is only of academic interest as it is not responsible for ultimate failure of the band. Figure 9 identifies the point on the band where large plastic strains ε_{pr} will lead to substantial band deformations and hence joint failure. This point stays the same for all models used in this analysis work and as shown in industrial applications of band clamps [12], is very likely to be in the region where a crack through the whole thickness of the band clamps starts to develop. Although the two graphs in Figure 10 seem to differ slightly, they still indicate the same tendency of plastic strain development. Again the plastic strain increases as the element size in this region has been reduced. The results for the structured mesh seems to be slightly more reliable because the element thickness along the whole inside of the band clamp was reduced whereas for the free mesh only the element size along the contact surface was decreased.

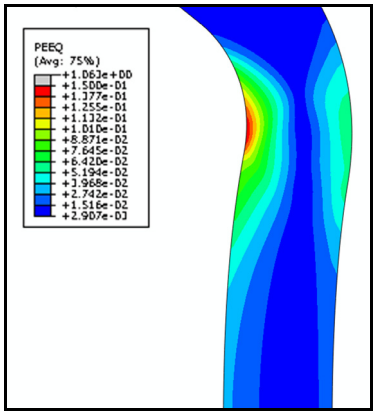

Figure 9: Position of maximum plastic strain sampling point for Figure 10

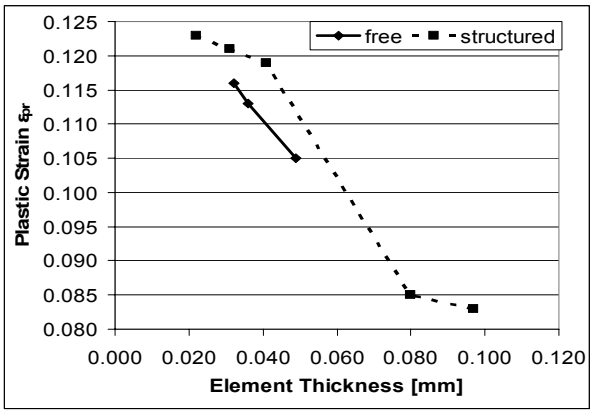

Figure 10 Maximum plastic strain taken from end point of radius for R = 0.3 mm and μ = 0.3.

4. Comparison of Explicit and Implicit Analysis

In this section the analyses for contact edge radii R = 0.1, 0.3 and 0.5 mm along with coefficients of friction μ = 0, 0.15 and 0.3, with a flange diameter D_f = 111 mm will be discussed and compared. The analyses were each solved using explicit and implicit solvers. The time periods for applying load were taken from an initial frequency analysis of the band where the first natural frequency f_n was predicted to be about 6850 cyc/time. The corresponding time period was t_n = 0.000146 sec, which in this paper is referred to as normal time. Time periods ten and fifty times slower (t_{10} = 0.00146 sec and t_{50} = 0.0073 sec) were also used.

4.1. Explicit Analysis Mesh Structure

Figures 11a and b show models that have reached the full failure state having the two extreme cases of very small radius R = 0.1mm combined with a very high coefficient of friction μ = 0.3, and a model with a relatively large radius R = 0.5mm and μ = 0.3, using an explicit solver. As can be seen in a) the small radius and high friction create a large distortion of the elements along the contact surface of the band clamp generating large plastic strain ε_{ps} = 180 whereas in b) the contact surface seems to be deformed as expected with a maximum plastic strain of ε_{ps} = 0.934, which seems very much more realistic. This demonstrates that the reliability and accuracy of the explicit analyses is highly dependent on the contact edge radius. During this analysis work it has been experienced that a higher edge radius R results in a more stable solution giving more realistic results.

As can be seen in Figure 12a and b also the coefficient of friction has a significant influence to the accuracy of the results. Figure 12b indicates that for the same contact edge radius R = 0.3 the higher coefficient of friction μ = 0.3 results in significantly deforming the elements along the contact surface and giving too large plastic strain results.

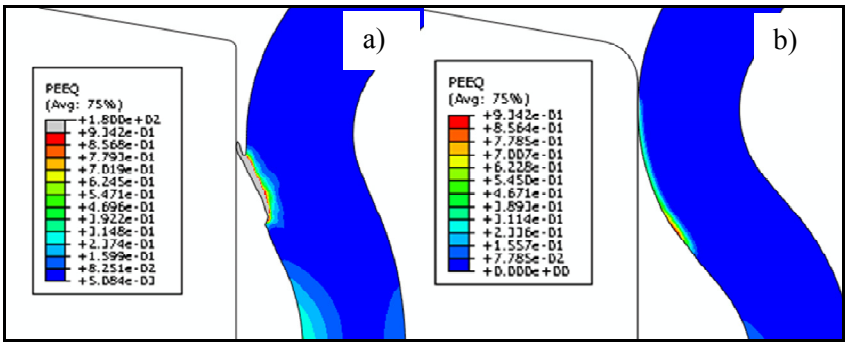

Figure 11: Full failure state using explicit solver and free mesh, 10 times slower a) R=0.1 mm μ = 0.3 and b) R = 0.5 mm μ = 0.3

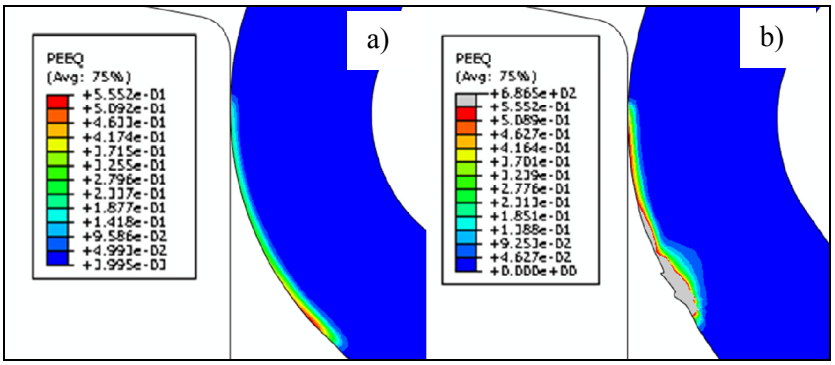

Figure 12: Model of V-section band clamp reached full failure mode using explicit solver for free mesh, 50 times slower a) R = 0.3 mm μ = 0 and b) R = 0.3 mm μ = 0.3

Several explicit analyses have shown that the type of mesh had only a slight effect on the accuracy of the results. Comparing the maximum plastic strain values along the contact surface of two explicit models, the strain values are nearly the same for both. This proofs that the mesh type does have almost no effect for a time t_{10} on the accuracy of the results generated.

As obtained in this subsection the results for contact in an explicit analysis highly depend on the radius of the rigid master surface (flange), the coefficient of friction, whereas the mesh type has no significant influence.

4.2. CPU (Run) Time

All analyses using an implicit solver and a free mesh were always running faster than their explicit counterpart which was set to run 10 times slower. Moreover the run time for the explicit solver increases as the mesh was changed from free to structured. This increase was due to an increase of elements as for the free mesh only the elements along the sliding surface were kept small and getting bigger the more they were away from this surface and for the structured mesh all elements in the model were kept the same size as at the contacting surface.

4.3. Reliability of Results

In Table 1 all explicit and implicit results for the models with a flange diameter $D_f = 111$ mm are compared, for contact edge radius R = 0.5 mm, all possible coefficients of friction and 10 times slower for the explicit.

As stated in the subsection before the CPU time increases a lot as the mesh density gets finer but comparing the results for ε_{pr} to the implicit results there is no significant difference. The results obtained here along with the results from both subsections before support the knowledge of the accuracy and reliability increasing as the coefficient of friction decreases and the contact edge radius R increases. The mesh type for explicit analyses has only a slight influence on accuracy but significantly increases the CPU time.

Table 1: Comparison of implicit and explicit solver for flange diameter D_f = 111 mm.

Contact Edge Radius R [mm]	Coefficient of Friction μ	Max. Plastic Strain at Corner End ε_{pr}	Mesh Type	Load Time (only for Explicit)	Solver Type	CPU (Run) Time [min]
0.5	0.3	0.1381	free	---	Implicit	9.0
0.5	0.3	0.1512	free	10	Explicit	19.0
0.5	0.3	0.1519	structured	10	Explicit	32.0
0.5	0.15	0.1021	free	---	Implicit	9.5
0.5	0.15	0.1182	free	10	Explicit	14.0
0.5	0.15	0.1183	structured	10	Explicit	31.0
0.5	0	0.0773	free	---	Implicit	9.2
0.5	0	0.0804	free	10	Explicit	14.0
0.5	0	0.0812	structured	10	Explicit	30.0

5. Conclusion

In this paper a model capable of predicting the ultimate axial load capacity and structural deformation of V-band Clamps using finite element analysis has been generated. It has been shown that the accuracy of analyses using implicit and explicit solver were highly depending on the contact edge radius R. Moreover the coefficient of friction μ had a significant influence on the stability of implicit analyses. Using explicit or implicit solver for contact analysis the contacting radius should be smooth enough. The accuracy of the results also depended on the element size and amount of elements along the sliding contact surface. Moreover the results were found to be depending on the type of mesh.

6. Further Work

The work presented in this paper has provided an understanding of how a model should be set up to investigate the ultimate axial load capacity of V-section band clamps. In further work the model should be improved to predict the interplay of elastic and plastic deformation mode, taking into account the influence of several V-band diameters.

References

[1] Shoghi K 2003 Stress and Strain Analysis of flat and V-section band clamps *PhD Thesis* Huddersfield
[2] NASA 2000 *Marman clamp system design guidelines*. Guideline GD-ED-2214, Goddard Space Flight Centre
[3] Shoghi K, Barrans S M, Rao H V 2004 Stress in V-section band clamps *Proceedings of the Institution of Mechanical Engineers* **218** 251-261
[4] Shoghi K, Barrans S M, Rao, H. V. 2003 Classical and finite element analysis of V-band retainers *NAFEMS World Congress* (Orlando Florida)
[5] Shoghi K, Barrans S M, Ramasamy P 2006 Axial load capacity of V-section band clamp joints *8th International Conference on Turbochargers and Turbocharging* (London) pp273-285
[6] Dassault Systemes 2007 Getting Started with Abaqus, v6.7 Section 12.4
[7] Konter A 2000 *How to Undertake a Contact and Friction Analysis* (Glasgow: NAFEMS) p 12
[8] Konter A 2005 *Advanced Finite Element Contact Benchmarks* (Glasgow: NAFEMS) p 19
[9] Dixit P M and Dixit U S 2008 *Modeling of Metal Forming and Machining Processes by Finite Element and Soft Computing Methods* (London: Springer) p 101
[10] Meyers M A and Chawla K K 1999 *Mechanical Behavior of Materials* (London: Prentice-Hall International UK Ltd) p 116
[11] Getting Started with Abaqus 2007 v6.7 Section 12.4 Dassault Systemes
[12] Brown I 10-12-2008 Teconnex Ltd. Keighley UK personal conversation